Journal of the Korean Chemical Society
2007, *Vol. 51, No. 2*
Printed in the Republic of Korea

수증기 쪼임법에 의한 제올라이트형 보로실리케이트 제조방법

R. Mansour*, M. Lafjah, F. Djafri, and A. Benguedach
Laboratoire de Chimie des Matériaux, Faculté des Sciences, Université d'Oran BP 1524 El-Menouer, 31000-Oran, Algeria (DZ)
(2006. 11. 18 접수)

Synthesis of Borosilicate Zeotypes by Steam-assisted Conversion Method

R. Mansour*, M. Lafjah, F. Djafri, and A. Benguedach
Laboratoire de Chimie des Matériaux, Faculté des Sciences, Université d'Oran BP 1524 El-Menouer, 31000-Oran, Algeria (DZ)
(Received November 18, 2006)

요 약. 펜타실 구조와 유사한 제올라이트형 결정성 보로실리케이드를 수증기 쪼임법으로 제조하였다. 실제 여러 종류의 서로 다른 붕소화합물 원료를 사용하여 만든 다양한 조성의 $Na_2O.SiO_2.B_2O_3.TBA_2O$ 겔을 건조시켜 얻은 무정형 분말을 수열합성 분위기에서 수증기를 쪼임으로써 펜타실 구조를 갖는 보로실리케이트 제올라이트를 합성하였다. 이때 MFI와 MEL 구조가 90:10의 비율을 혼합되어 있는 새로운 중간구조 물질이 얻어 졌다. 본 연구로부터, 젖어 있는 반응성 고체상 물질이 수증기와 높은 pH 분위기에서 결정화가 아루어짐을 확인하였다. X-선 회절법으로 분석한 결과 생성물은 우수한 결정성을 가질뿐만 아니라 독특한 촉매적 성질을 보일것으로 예상되는 구조를 갖는다. 또한 반전중심을 갖는 MFI 구조의 펜타실 층이 규칙적으로 쌓이는 모양을 보이지만 이는 MEL 구조의 거울상 층으로 이루어진 결함에 의해 방해된다. 생성물은 77 K 질소흡착법에 의하면 미세기공 부피가 0.160 cc/g 로서 순수한 MFI 구조 물질이 갖는 0.119 cc/g 보다 더 크며, 비교적 넓은 비표면적(~600 m^2/g)을 보인다. 적외선 스펙트럼에서는 900.75 cm^{-1}에서 흡수띠를 보이는데, 이는 붕소가 결정성 실리케이트의 사면체 구조내에 위치함을 뜻한다.

주제어: 보로실리케이드, 구조지향물질, MFI, MEL, 펜타실구조, 상호성장, 건조겔법, 수증기쪼임법

ABSTRACT. Intermediate pentasil borosilicate zeolite-like materials have been crystallized by a novel method named steam-assisted conversion, which involves vapor-phase transport of water. Indeed, amorphous powders obtained by drying $Na_2O.SiO_2.B_2O_3.TBA_2O$ gels of various compositions using different boron sources are transformed into crystalline borosilicate zeolite belonging to pentasil family structure by contact with vapors of water under hydrothermal conditions. Using a variant of this method, a new material which has an intermediate structure of MFI/MEL in the ratio 90:10 was crystallized. The results show that steam and sufficiently high pH in the reacting hydrous solid are necessary for the crystallization to proceed. Characterization of the products shows some specific structural aspects which may have its unique catalytic properties. X-ray diffraction patterns of these microporous crystalline borosilicates are subjected to investigation, then, it is shown that the product structure has good crystallinity and is interpreted in terms of regular stacking of pentasil layers correlated by inversion centers (MFI structure) but interrupted by faults consisting of mirror-related layers (MEL structure). The products are also characterized by nitrogen adsorption at 77 K that shows higher microporous volume (0.160 cc/g) than that of pure MFI phase (0.119 cc/g). The obtained materials revealed high surface area (~600 m^2/g). The infrared spectrum reveals the presence of an absorption band at 900.75 cm^{-1} indicating the incorporation of boron in tetrahedral sites in the silicate matrix of the crystalline phase.

Keywords: Borosilicate, Structure Directing Agent, MFI, MEL, Pentasil, Intergrowth, Dry Gel Method, Steam-assisted Method

INTRODUCTION

Crystallization of MFI-type structure zeotype materials with a trivalent metal present in tetrahedral (T) positions has had a tremendous impact in synthesis of new shape selective industrial catalysts having tunable acidic strength.[1] Thus, the isomorphous substitution of Si by other tetrahedrally coordinated heteroatoms such as B(III) provides new materials showing structural modifications and specific catalytic properties, namely cracking of olefins with 95% of propylene as product and conversion of heavy hydrocarbons into gasoline, BTX and other important aromatic products.[2-5] However, crystallization of a borosilicate zeotype with MFI/MEL structure, having a three dimensional medium pore system of a 10-membered ring, confers its unique characteristics.

The most common method for preparing zeolites is the conventional hydrothermal synthesis (HTS). The new synthetic method for zeolites and zeotypes, in which an aluminosilicate gel dried in advance is crystallized into a zeolitic phase in a gas environment, has been developed and named dry gel conversion (DGC).[6-9]

In 1990, Xu *et al.*[17] introduced a new technique, in which they converted an amorphous aluminosilicate in contact with steam and vapors of volatile amines into ZSM-5 zeolite. This technique has been referred to as the vapor-phase transport method (VPT). If non-volatile quaternary ammonium ions are used as templates, then only water vapor is supplied via the gas phase; therefore the method is rather named steam-assisted conversion (SAC).[10,18] The SAC method enables us to achieve rapid and full crystallization of an amorphous dry gel, which contains tetraalkylammonium cations, into a crystalline zeotype phase.[15]

Synthesis of high silica borosilicate zeotype by steam assisted conversion method was first reported by Banyopadhyay *et al.*[6] In his study, synthesis and characterization of [B]-MFI,-BEA and -MTW phases were investigated using tetraethylammonium cations. Clearly, due to the different conformations of TEA^+ entrapped in divergent host lattices, the three phases have been obtained as it was shown by Curtis *et al.*[12] It is obvious that organic templates are a powerful tool in synthesis of high silica zeolites having high stability, however, their role has not been completely understood yet since we are still not able to predict what structures will produce a particular organo-cation template in different synthesis conditions, and this is due mainly to the very complex guest/host relationships.[17]

Moreover, Song-Jong Hang[13] has successfully synthesized new high silica zeolite structure SSZ-47 using a mixture of quaternary ammonium cations, so it has been showed that they still have high potential and possibility to produce novel structures. Even though they were used by Barrer *et al.*[14] in the early 1960s, they result in the discovery of numerous new zeolitic structures yet.

In the present study, we have explored, via the X-ray investigation based on powder diffraction data and other techniques, the phase nature of the materials obtained when using the TBA^+ cations as structure directing agent under the new synthesis conditions of the SAC method.

EXPERIMENTAL

Synthesis of materials

The following reagents have been used for the synthesis of zeoborosiles (borosilicate zeolites): sodium hydroxide NaOH (Aragonesas 99.99%), boric acid H_3BO_3 (Labosi 99.5%), triethylborate $(C_2H_5O)_3B$ (Aldrich 99%), borate sodium $Na_2B_4O_7.10H_2O$ (PANREAC 99.5%), colloidal silica SiO_2 (Ludox-HS-40 Dupont, 40 wt.%), and tetra-n-butylammonium hydroxide $C_{16}H_{37}NO$ (MERCK 20%).

The synthesis of borosilicate zeotypes was performed following the general dry gel conversion technique described elsewhere.[6,8,16] For this method amorphous solid oxide powders were prepared as follows, an appropriate amount of tetralkylammonium hydroxide was mixed with a silica source, and the mixture has been stirred for 10 min. Boron source was dissolved in deionised water and added to the above mixture and the final mixture was further stirred for 2 hours. Then, the gel was dried at

80-90 °C over an oil bath with continuous stirring allowing evaporation of water. When the gel became thick and viscous, it was homogenized by hand using a teflon rod until it dried, so a white solid was formed. It was ground into a fine powder and was poured into a small teflon cup. This cup was placed in a teflon-lined autoclave (65 ml) with water which was the source of steam. The dry gel never came into the direct contact with water. The autoclaves were heated in forced convection ovens for prescribed times at 175 °C in autogeneous pressure. After the crystallization period was over, the autoclaves were quenched with cold water and the zeoborosile samples were taken out from the cups, filtered and washed thoroughly with distilled water, and dried overnight at 100 °C.

Heat treatment

The removal of organic template occluded inside the borosilicate zeolite pores was carried out by a heat treatment. The as-synthesized samples were placed in a muffle furnace and heated stepwise in a flow of nitrogen. The temperature was raised to 550 °C over a period of 4 hours and kept at the same temperature for 4 hours. The temperature was then raised again to 600 °C over a period of 4 hours and kept again at this temperature for another 4 hours and finally the sample was cooled to room temperature.

Characterization

X-ray powder diffraction (XRD) patterns were collected on a Philips PW 1830 diffractometer (CuKα: λ=1.5406 Å, 40 kV, 20 mA). KBr pellet technique was used to perform FT-IR spectroscopy of the samples using a Nicolet 460 FT-IR spectrometer; the samples were ground with KBr and pressed into thin wafers. Nitrogen adsorption isotherms were collected at 77 K on Micrometrics Gemini II 2370 area analyser. The degassing and activation pre-treatment was carried out at 673 K for 4 h prior to the analysis.

RESULTS AND DISCUSSION

Optimal chemical composition of the reaction gel

Crystallization of borosilicate zeotypes from borosilicate gels containing sodium and TBA^+ cations by steam-assisted crystallization method has not been reported yet, however, there are only some recipes for preparation of zeoborosiles using other quaternary cations as templates in the literature. Comparative data on these recipes in terms of molar ratios of components in gel are listed below (see *Table* 1). In this study, the optimal molar composition of gel is as follows:

$$SiO_2 : 0.042\ Na_2O : 0.0125\ B_2O_3 : 0.098\ TBA_2O$$

X-ray powder diffraction

The X-ray diffraction patterns of the borosilicate powder (dry gel) and as- synthesized borosilicate

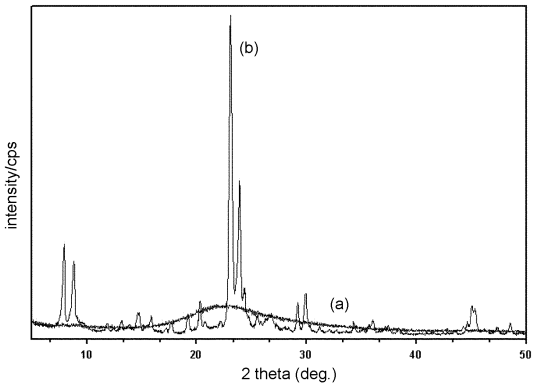

Fig. 1. XRD patterns of (a) amorphous borosilicate (b) crystalline borosilicate.

Table 1. Molar compositions of some zeoborosiles in the literature

Reference	SiO_2/B_2O_3	OH^-/SiO_2	Na_2O/SiO_2	Boron Source
Mansour *et al.* MFI/MEI.	80	0.28	0.042	H_3BO_3
Rubin *et al.* MFI (1991) [38]	130	0.51	0.25	H_3BO_3
Hinnenkamp *et al.* MFI (1983)[33]	12-50	0.20-0.90	0.4-1.8	H_3BO_3
Klotz *et al.* MFI (1981)[31]	101-150	0.1-2	0.2-4	H_3BO_3
Bandyopadhyay *et al.* BEA (1999)[6]	30-200	0.416-1.3	0.028-0.05	$Na_2B_4O_7$
Z-Y. Yuan *et al.* MYW (1999)[37]	100-300	0.1-0.25	-	H_3BO_3

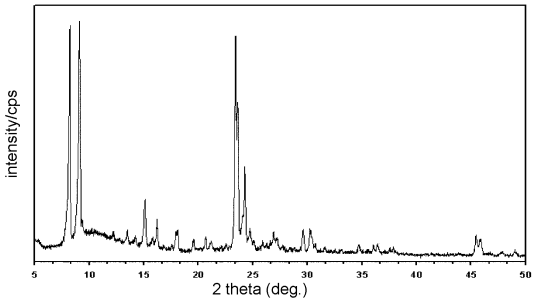

Fig. 2. XRD Pattern of [B]-MFI/MEL (calcined sample).

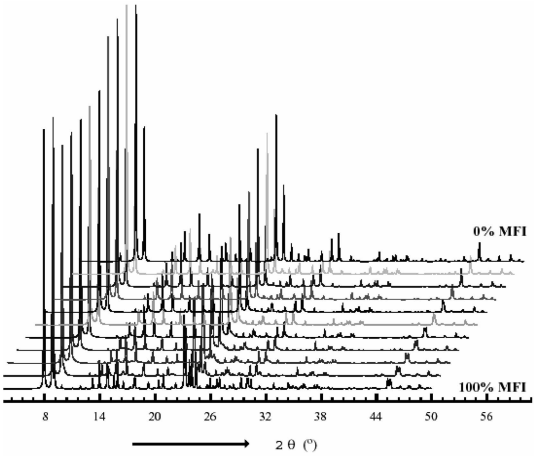

Fig. 3. Simulated XRD patterns for MFI-MEL series [21].

materials are shown in *Fig.* 1. The XRD pattern of the calcined sample is shown in *Fig.* 2. The data presented in both figures shows that both of the materials calcined and as-synthesized samples obtained using tetrabutylammonium cations (TBA) as template were highly crystalline: The XRD patterns in this work were identified to be one of the MFI-MEL intermediates family (see *Fig.* 3).

The reticular distances d_{hkl} of our materials are higher than those of pure MFI zeolites as shown in *Table* 2, and this leads us to suggest that our product has a different and specific structure. The apparent topology is that of MEL since there exist two peaks between 2θ–8-9° and two others at 2θ–23-24° much more intense (see *Fig.* 1). However, the appearance of two weak peaks at 2θ–45° usually characterizing the MFI structure has led us to proceed to a higher resolution (0.007). We tried to

Table 2. Principal reticular distances of prepared zeoborosiles and simulated zeolite

hkl	d (ZSM-5) [Al]-MFI	d [B]-MFI/MEL	d(AMS-1B) [B]-MFI
101	11.126	11.153	11.030
200	10.011	10.023	9.898
111	9.971	- diff.	9.685
501	3.836	3.849	3.818
051	3.814	- sup.	- sup.
151	3.747	- diff.	3.729
303	3.708	3.723	3.695
133	3.640	3.654 diff.	3.625

identify and localize all the peaks characterizing the MFI structure and we have found some peaks are dramatically diffused according to the absence conditions, in particular the reflections of planes (151) and (133) and others are found to be superimposed, namely reflections of planes (501) and (051), (see *Table* 2). By comparison with *Fig.* 3, the structure of the product is supposed to be an intergrowth of two topological structures MFI and MEL in the ratio (90% MFI and 10% MEL).[21]

Infrared spectroscopy

Midinfrared spectroscopic studies of the zeolite framework vibrations in the framework region have been widely used to characterize and to differentiate various zeolite structures. *Fig.* 4 revealed the FT-IR spectra of framework vibrations in the 1400-400 cm^{-1} range of the three as-synthesized zeosili-

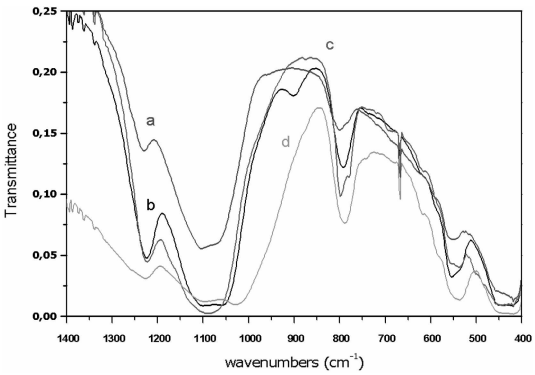

Fig. 4. Midinfrared spectra of samples with MFI/MEL structure of (a) as-syn. silicalite, (b) as-syn. borosilicate (c) calcined borosilicate and (d) as-syn. aluminosilicate (zeolite).

cate versions, namely zeosile, zeolite and zeoborosile with (Si_2O/B_2O_3 or Si_2O/Al_2O_3=80) as well as the calcined borosilicate version. Several IR bands are observed at 1224, 792 and 550 cm^{-1}. Two Large bands at 1080 and 440 cm^{-1} and shoulder at 580 cm^{-1} are also observed. As to as-synthesized borosilicate sample, it should be noted that there are one additional IR band at 900.75 cm^{-1} and two shoulders at 781 and 536 cm^{-1}.

The band at 550 cm^{-1} is characteristic of ZSM-5 (MFI), while absorption band at ~ 450 cm^{-1} is common to pentasil zeotypes and amorphous silicates. Zeolites that contain five-membered rings (pentasil structure) usually present IR bands at 1220 and 560 cm^{-1}.[40]

The intense IR band at 1220 cm^{-1} was assigned to the extensive asymmetric stretching vibrations of the framework (four chains of five-membered rings for the pentasile family), while the IR band at 560 cm^{-1} was attributed to the double five-membered ring blocks and it is sensitive to the topology and building units of the zeolite frameworks. This band was observed at 580 cm^{-1} in mordenite (MOR) which is a large-pore zeolite. However, the additional absorption band at 900.75 cm^{-1} is observed, but Bandyopadhyay *et al.*[6] observed the absorption bands at 930 cm^{-1} and 1397 cm^{-1} which were attributed to the symmetric and asymmetric stretching vibrations of B-O-Si group.[41] In our spectra, the absorption band at 1397 cm^{-1} is not observed It should be noted that the presence of the band at 900.75 cm^{-1} only in the borosilicate version *Fig.* 4(b) confirms the incorporation of boron atoms and it is due to framework vibrations of tetrahedral entities $B(OSi)_4^-$[6] and it could be attributed to the stretching of the Si-O-B bond.[44] On the other hand, the presence of a shoulder at 586 cm^{-1} may be attributed to the double five-membered ring blocks vibrations sensitive to the particular structure of the intergrowth of both MFI and MEL pore systems namely , the two types of pore system bi- and three dimensional channel systems.[37] The IR spectra reported in *Fig.* 4 are in agreement with the pentasil structure type confirmed by the XRD data. We notice that the large absorption band of the zeolitic sample is moved towards smaller wavenumbers compared to the zeosile and the zeoborosile samples.

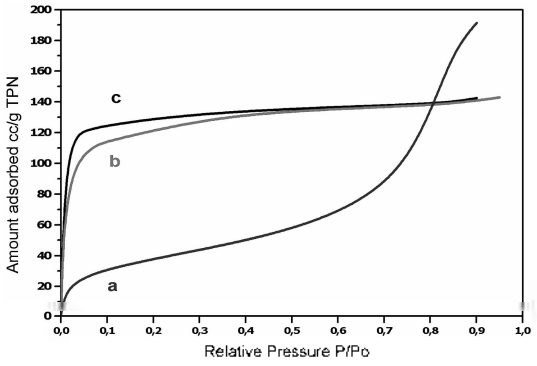

Fig. 5. Nitrogen adsorption on (a) amorphous borosilicate (b) [B]-MFI and (c) [B]-MFI/MEL.

Nitrogen adsorption measures at 77 K

Fig. 5 illustrates the nitrogen adsorption isotherms from the starting oxide powder and the solids (MFI and MFI/MEL) obtained from the SAC method after calcination in nitrogen flow at 550 °C and then 600 °C to remove tetrabutylammonium cations.

Nitrogen adsorption at 77 K allowed us to discuss the texture of the amorphous sample *Fig.* 5(a) and it indicates that the amorphous solid adsorbs nitrogen at low P/Po values indicating the presence of pores in the same range as the crystalline samples *Fig.* 5(b) and (c). However, the porous structure of the sample is dramatically different and shows an isotherm of type II and this means the adsorption took place on non-porous powders or powders with pores diameters higher than micropores (pores of 20Å diameter or less).[36,42] The inflexion point of the isotherm usually comes near the complete filling of the first adsorbed monolayer and along with the increase of relative pressure; the following layers are filled till the number of layers be infinite. Moreover, there is some resemblances to isotherm of type IV where there exist pores with radii 15-1000 Å, which confirms the presence of micropores in the borosilicate dry gel.[43] The adsorption isotherms in *Fig.* 5(b) and (c) of the samples [B]-MFI/MEL and [B]-MFI show the typical isotherm of type I characterizing

Table 3. Textural Characteristics of Samples

Sample	Volume	Surface		
	Micropores ($cm^3\ g^{-1}$)[a]	BET ($m^2\ g^{-1}$)[b]	Langmuir ($m^2\ g^{-1}$)[c]	Ext. ($m^2\ g^{-1}$)
Borosilicate (Amorphous)	---	133.14	227.63	150.37
Zeoborosile (MFI/MEL)	0.1603	397.61	586.03	88.18
Zeoborosile (MFI)	0.1197	416.55	572.07	155.00

[a]t-plot method
[b]specific area measured by Brunauer-Emmet-Teller (BET) method
[c]specific area measured by Langmuir Method

the microporous structures. The adsorption capacity of the product [B]-MFI/MEL presumably larger than that of the product [B]-MFI because of the increased crystallinity and porosity. The BET and Langmuir surface areas of the samples with SiO_2/B_2O_3=80 measured at liquid nitrogen temperature are listed above in *Table* 3.

The textural data draw attention to the fact that the sample [B]-MFI/MEL shows higher microporosity (0.160 cc/g) than that of the pure phase [B]-MFI (0.119 cc/g), which is probably attributed to the larger cages of MEL structure.[45] Also, it should be noted that the external surfaces are different and consequently the crystal size and the form of crystals are likely to be different too.

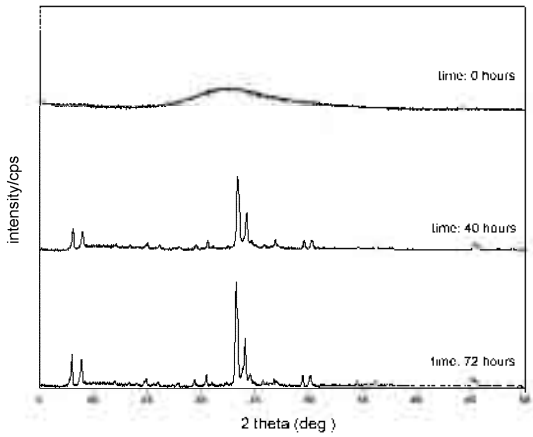

Fig. 6. XRD patterns of products using TBA as template after different periods of crystallization (0-72 hours).

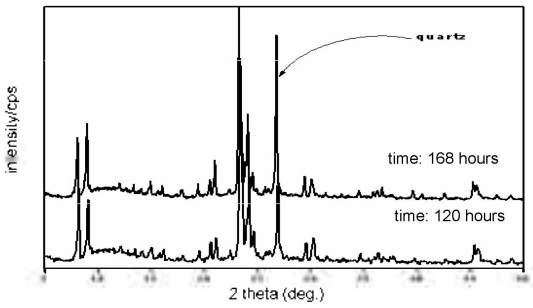

Fig. 7. XRD patterns showing partial conversion of the zeo-phase (MFI/MEL) into quartz after 100 hours.

Crystallization Process

It should be pointed out that from a thermodynamic viewpoint the majority of known zeolites constitute metastable phases. Under the influence of various synthesis parameters, they may undergo further changes such as recrystallization into phases with slightly lower free energy. This explains the strong dependence of the hydrothermal synthesis of zeolites upon numerous kinetic parameters.[19] In spite of the fact that the size and the shape of the guest molecules often correlate well with the void dimensions within the host, there are still aspects of phase selectivity in zeolite synthesis that are kinetically controlled, so that the same organo-cation guest may be capable of crystallizing more than one zeolitic phase.[27] For this reason, following the crystallization process is of most importance. Thus, the time evolution of the sample with SiO_2/B_2O_3=80 has been investigated. The experiment was performed at 175 °C and autogeneous pressure. *Figs*. 6 and 7 show the XRD patterns obtained from the solid phases collected at various time intervals (40 h, 72 h, 120, and 168 h.). Initially, the dry gel is essentially amorphous. After only 40 hours of heating the sample is mainly highly-crystalline zeolite and at first it shows a strong similarity to that of zeolites ZSM-11 (MEL).[21-29] As mentioned above our product consists of an intergrowth of two pentasil phases,

namely 10% MEL and 90% MFI. It should be noted that after a crystallization period of 100 hours, the XRD patterns start to show the appearance of peaks characterizing the phase of quartz. Henceforth, the prolongation of time of crystallization has led to the total conversion of the zeophases into quartz phase, which is the most stable phase.

CONCLUSION

The present steam-assisted crystallization technique is an effective method for the synthesis of an intermediate pentasile zeoborosile with an intergrowth type of (10% MEL/ 90%MFI). This type of intergrowth is thought to be a very stable phase when varying the space parameters; however, it is an unstable kinetic phase. This material show higher cristallinity and higher microporosity compared to pure MFI-type zeoborosile owing to the presence of larger cages of MEL structure. On the other hand, the presence of band absorption at ~900 cm^{-1} indicates the incorporation of boron atoms in the silicate matrix of the products compared to other versions.

REFERENCES

1. Aiello, R.; Nagy, J.B.; Giordano, G.; Katovic, A.; Testa, F. *C. R. Chimie.* **2005**, *8*, 321-329.
2. Coudurier, G.; Auroux, A. J.; Vedrine, C.; Farlee, R.; Abrams, L.; Shannon, R.D. *J. Catal.* **1987**, *1*, 108.
3. Millini, R.; Perego, G.; Bellussi, G. *Top. Catal.* **1999**, *9*, 13.
4. Alexander, B. D. *US 20 020 004 624*, **2002**.
5. Chen, C-Y. *US 20 030 133 870*, **2003**.
6. Bandyopadhyay, R.; Kubota, Y.;Sugimoto, N.; Fukushima Y.; Sugi, Y. *Microp. Mesop Mater.***1999**, *32*, 81.
7. Bandyopadhyay, R.; Kubota, Y.; Ogawa, M.; Sugimoto, N. N.; Fukushima Y.; Sugi, Y. *Chem. Lett.*, **2000**, 300.
8. Rao P. R. H. P.; Matsukata, M. *Chem. Commun.*, **1996**, 1441.
9. Rao, P. R. H. P.; Uyema K.; Matsukata, M. *Appl. Catal.* **1998**, *166*, 97.
10. Matsukata, M.; Ogura, M.; Osaki, T.; Rao, P. R. H. P.; Nomura, M.; Kikuchi, E. *Topics Catal.* **1999**, *9*, 77.
11. Tatsumi, T.; Jappar, N. *J. Phys. Chem.*, **1998**, *102*, 7126.
12. Brand, H. V.; Curtis, I. A.; Iron, L. E.; Trouw, F. R.; Brun, T. B. *J. Phys. Chem.* **1994**, *98*, 1293.
13. Huang, S-J.*Chemestry of Materials*, **2002**, *14*, 313-320.
14. Barrer, R. M. *hydrothermal chemistry of zeolites*, Academic Press, London, **1982**.
15. Matsukata, M.; Osaki, T.; Ogura, M.; Kikuchi, E. *Microp. Mesop Mater.* **2002**, *56*, 1-10.
16. Tatsumi, T.; Jappar, N. *J. Phys. Chem. B.* **1998**, *102*, 7126-7131.
17. Xu, W.; Dong, J.; Li, J.; Li W.; Wu, F. *J. Chem. Soc. Chem. Commun.* **1990**, 755.
18. Arnold, A.; Hunger, M.; Weitkam, J. *Microp. Mesop. Mater.* **2004**, *67*, 205-21.
19. Cichoki, A.; Kscielniak, P. *Microp. Mesop. Mater.* **1999**, *29*, 369-382.
20. Wagner, P.; Nakagawa, Y.; Lee, G. S.; Davis, M. E.; Elomari, S.; Medrud, R. C.; Zones. S. I. *J. Am. Chem. Soc.*, **2000**, *122*, 263-273.
21. http://www.iza-structure.org/databases.
22. Kokotailo, G. T.; Chu, P.; Lawton S. L.; Meier, W. M. *Nature*, **1978**, *275*, 119-120.
23. van Koningsveld, H.; den Exter, M. J.; Koegler, J. H.; Laman, C. D.; Njo S. L.; Graafsma, H.*Proc.12 th Int. Zeolite Conf. IV*, **1999**, 2419-2424.
24. Perego G; Cesari, M. *J. Appl. Crystallogr.* **1984**, *17*, 403-410.
25. Taramasso, M.; Manara, G.; Fattore V.; Notari, B. *GB 2 024 790*, **1980**.
26. Bibby, D.M.; Milestone N.B.; Aldridge, L.P.*Nature*, **979**, *280*, 664-665.
27. Terasaki, O.; Ohsuna, T.; Sakuma, H.; Watanabe, D.; Nakagawa, Y.; Medrud, R.C. *Chem. Mater.* **1996**, *8*, 463-468.
28. Nakagawa, Y.; Dartt, C. *US Patent. 5 968 474*, **1999**.
29. Reddy, J.S.; Kumar, R. *Zeolites*, **1992**, *12*, 95-100.
30. Kokotailo, G.T.; Lawton, S. L.; Olson D. H.; Meier, W. M. *Nature*, **1978**, *272*, 437.
31. Klotz, M. R. *US 4 269 813*, **1981**.
32. Taramasso, M.; Manara, G.; Fattore V.; Notari, B. *GB 2 024 790*, **1980**.
33. Hinnenkamp, J. A.; Walatka, Jr.; Vernon V.; *US 4 423 020*, **1983**.
34. Taramasso, M.; Perego G.; Notari, B.; *In Proc. 5th Int. Zeolite Conf.*, **1980**, 40-48.
35. van der Gaag, F. J.; Jansen J. C.; van Bekkum H.; *Appl. Catal.*, **1985**, *17*, 261.
36. Mathaway P.E.; Davis, M. E. *Catal. Lett.* **1990**, *5*, 333.
37. Yuan, Z.-Y.; Chen, T.-H.; Long, Z.-B.; Wang, J.-Z.; Li. H.-X. *12th International Zeolite Conference, Materials Research Society*, **1999**, 1655.

38. Rubin et al. *US Patent 5 063 037* **1991**.
39. Ione, K. G.; Vostrikova, L. A.; Mastikhin, V. M. *J. Mol. Catal.* **1985**, *31*, 355.
40. Ngokoli-Kekele, P.; Springuel-Huet, M.-A.; Man, P.; Thoret, J.; Fraissard, J.; Corbin, D. R. *Microp. Mesop. Mater.* **1998**, *25*, 35-41.
41. Szostak, R. *Molecular Sieves: Principles of Synthesis and Indentification*, Blackie Academic and Professional Van Nostrand Reinhold, New York, **1989**.
42. Kim, M.-H.; Li, H.-X.; Davis, M. E. *Microp. Mater.* **1993**, *1*, 191-200.
43. www.granuloshop.com/qc/sorption.htm.
44. Lobo, R. F.; Davis, M. E. *J. Am. Chem. Soc.* **1995**, *117*, 3766.
45. Thomas, J. M.; Bell, R. G.; Catlow, C. R. A. In *Handbook of Heterogeneous Catalysis*. Eds.: Ertl, G.; Knözinger, H.; Weitkamp J., Wiley, **1998**, p.303.